Section A-Research paper

NUMERICAL STUDIES OF SOLAR WATER HEATING SYSTEM WITH CPC SOLAR COLLECTOR AND THERMAL ENERGY STORAGE

C. Natesamurthi [a,*], S.Karthikeyan [a], Y.Robinson [a], K.Gopalakrishnan [b], J.Manivannan [a], Bibin K Jose [c]

[a] Department of Mechanical Engineering, Erode Sengunthar Engineering College, Perundurai, Erode-638057, India

[b] Department of Mechanical Engineering, K S R Institute of Engineering and Technology, Tiruchengode-637215, India

[c] PG and Research Department of Mathematics, Sanatana Dharma College, Alappuzha-688003, India

[*] Corresponding author email: cnmoorthi1975@yahoo.com

Abstract

Solar water heating (SWH) systems becomes increasingly popular in modern buildings, due to significant reduction in energy consumption in heating applications. In this work, an active SWH is modeled using TRNSYS software for climatic conditions of Chennai, India, employing an external compound parabolic concentrator solar collector (XCPCSC) and stratified thermal storage system (STESS).The performance parameters are estimated on the basis of monthly and annual averaged solar fractions (SF) by varying the collector area, mass flow rate, various controller strategies, STESS geometry. The simulated studies have specified the ability of the optimized system to supply the hot water demand of 280 $l\ d^{-1}$ at 60 °C, attaining a SF of 0.97. This design strategy can be implemented for the development of an efficient SWH system, utilizing zero energy consumption from conventional resources. The proposed TRNSYS model has been validated using experimental data under similar test conditions. An influence of placing XCPC under evacuated tubes is simulated, resulting 5% improvement in energy gained over an evacuated tube solar collector without XCPC.

KEYWORDS

CPC collector, evacuated tube, thermal energy storage, TRNSYS, solar water heating

1. INTRODUCTION

The sun produces energy at the rate of 3.8×10^{23} kW, of which the earth receives only 1.8×1014 kW (Kalogirou, 2014).The remaining energy is reflected in the atmosphere. When converting intercepted energy at an efficiency of 10 %, 0.1 % of the energy received by the earth from the sun's overall power producing ability would be four times that of the entire globe. This is equivalent to the output of one hundred million modern power stations (Hankins, 2012)[3]. Harnessing of solar energy depends mainly on its absorption and conversion into heat energy using a network of collectors. The most common solar thermal collectors are namely flat plate (FP), evacuated tube (ET), and concentrated solar collectors. Non-concentrated solar collectors, including ET and FP, exhibit relatively lower thermal efficiency as the temperature rises. Concentrated solar collectors, as against to non-concentrated solar collectors are appropriate for temperatures above 80°C(Li et al., 2016). High-concentrated solar collectors would fulfill energy requirements and need a tracking system, which adds to operational costs. A significant diffusion loss is encountered in these collectors, making them incompatible for low-temperature applications (Christopher et al., 2021). External compound parabolic concentrator solar collector (XCPCSC) is a non-imaging collector that can reflect the majority of incident radiation back to the absorber tube, attaining higher thermal efficiency compared to the non-concentrated solar collector (Kürklü et al., 2002).

A growing interest has been witnessed in the recent years on the modification of collector structure and incorporation of thermal energy storage system (TESS). Tchinda and Ngos(Tchinda and Ngos, 2006) reported the superior thermal performance of the CPC solar collector by selective observer surface over a black coated one. Their findings have revealed the higher effectiveness of the selective observer surface compared to the black painted absorber surface. Experimental studies of Gang et al(Gang et al., 2012) indicated a enhanced thermal performance of the ET- CPC collector through U-type absorber pipes, reaching HTF temperature of 90 °C suitable for the applications such

as desalination, space cooling etc. Sobhansarbandi and Atikol[6] made a comparison between FP and CPC solar collector and have reported an appreciable reduction in the collector area from 8 m^2 to 2 m^2, while using CPC solar collector in the place of FPC for attaining the same outlet HTF temperature. Liu et al(Liu et al., 2013)carried out experiments in a CPC solar collector with two different reflectors having a flat and involute shape. There was a 10–15 %decrease in the flat curve reflector over the other one with involute reflector as a result of an increase in the acceptance angle. A numerical study of Xu et al(Xu et al., 2020) showed a higher uniform distribution of solar radiation in multi sectioned CPC solar collector over a conventional CPC solar collector under the same conditions. Xia and Chen(Xia and Chen, 2020) performed experiments in an ET solar collector coupled to mini CPC reflector. An enhancement in thermal efficiency of 24.3 % - 29.2 % was reported over the conventional evacuated collector due the placement of mini CPC. Sokhansef at et al (Sokhansefat et al., 2018)studied thermo economic analysis of SWH system and reported a total rate of return around 74 % and 69 % using FPC and ET under same cold climatic condition.

The fluctuating availability of solar energy which widens the gap between demand and supply, is one of the most serious issues for any solar thermal system. This really requires dynamic matching of the SWH system that can be achieved through integration of TESS (Dinçer and Rosen, 2010).The stored thermal energy can be in the form of sensible or latent heat and directly retrieved in the form of hot or cold energy from the TESS, minimizing the losses associated with the energy conversion[11]. Sensible TESS (STESS) find extensive use in applications because of simpler in design, enormous availability of storage medium and least chance of thermal degradation, though their energy density is 3-5 times lower than the latent heat TESS. Thermal design of solar water heating (SWH) unit requires the forecast of useful energy gained with respect to geographical location and proper sizing of the different components. Eventually, it involves costlier experimentation and is time consuming.

With the recent advancements in computational tools, evaluatation of thermal performance of the proposed system is done under dynamic conditions using Transient System Simulation (TRNSYS) tool. Hobbi and Siddiqui(Hobbi and Siddiqui, 2009)optimized the SWH system using TRNSYS, reporting the SF of 0.83 - 0.97 and 0.30-0.62 during summer and winter seasons respectively. Replacement of non-selective material with selective one increased the annual SF from 0.54 to 0.69.Shrivastava et al(Shrivastava et al., 2017) have presented a critical review of TRNSYS components in SWH system that mainly include weather file, types of collector, storages and controllers. The local weather conditions have a large influence on the performance of SWH system and database are continuously being updated for new geographical locations ("TRNSYS primary," 2021). Different solar collector modules are available as components, circulating with HTF through natural or forced circulation. Proper selection of HTF can improve the performance and economic design of SWH system particularly used in ET. Arab and Abbas(Arab and Abbas, 2013) did analysis of thermal performance of SWH in housed hold located at Sydney in Australia. A groove type ET taken for the analysis exhibited higher performance through improvement in the properties of HTF. Effects of thermal stratification on SWH system were analyzed with respect to geometries, orientation, volume and position of inlet and outlet of storage tank (Antoniadis and Martinopoulos, 2019; Guédez et al., 2014).The reported results revealed the requirement of high degree of stratification for achievement of higher thermal performance in a passive manner, necessitating the appropriate selection of HTF flow and controller (Abdunnabia et al., 2014; Tiwari et al., 2020).

In view of the above stated fascinating features of the XCPCSC and the merits accrued with the integration of a STESS, it is proposed to carry out the simulation of SWH system under climatic conditions of Chennai. Initially, the simulated results have been compared with experimental data for validating the TRNSYS model. In continuation, a study of thermal behavior of the SWH system was made by varying the geometrical parameters, HTF flow rate and control system (variable speed

controller and hysteresis controller).An algorithm was developed for inclusion of variable flow controller for operation of the pump based on the outlet temperature of the heat transfer fluid (HTF).The effects of key parameters for attaining a maximum degree of thermal stratification in STESS and SF were explored.

2. SYSTEM DESCRIPTION

In this section, the experimental facility and TRNSYS model used in the study are described as follows;

2.1 Experimental test facility

Evaluation of thermal behavior of the SWH system was done at various experimental conditions using an experimental test facility. This setup consists of a XCPCSC, STESS, makeup HTF tank, pump and necessary measuring devices. A serpentine arrangement was made for interconnection between eight evacuated tubes (ET) in series, each having a diameter of 0.05 m and length of 1.8 m. A copper tube having 6 mm outer diameter and 1 mm thickness of wall spanned the length of each ET. Each ET was mounted on an aluminium reflector with a half acceptance angle of 55 ° and an aperture area of 0.15 m^2, respectively.

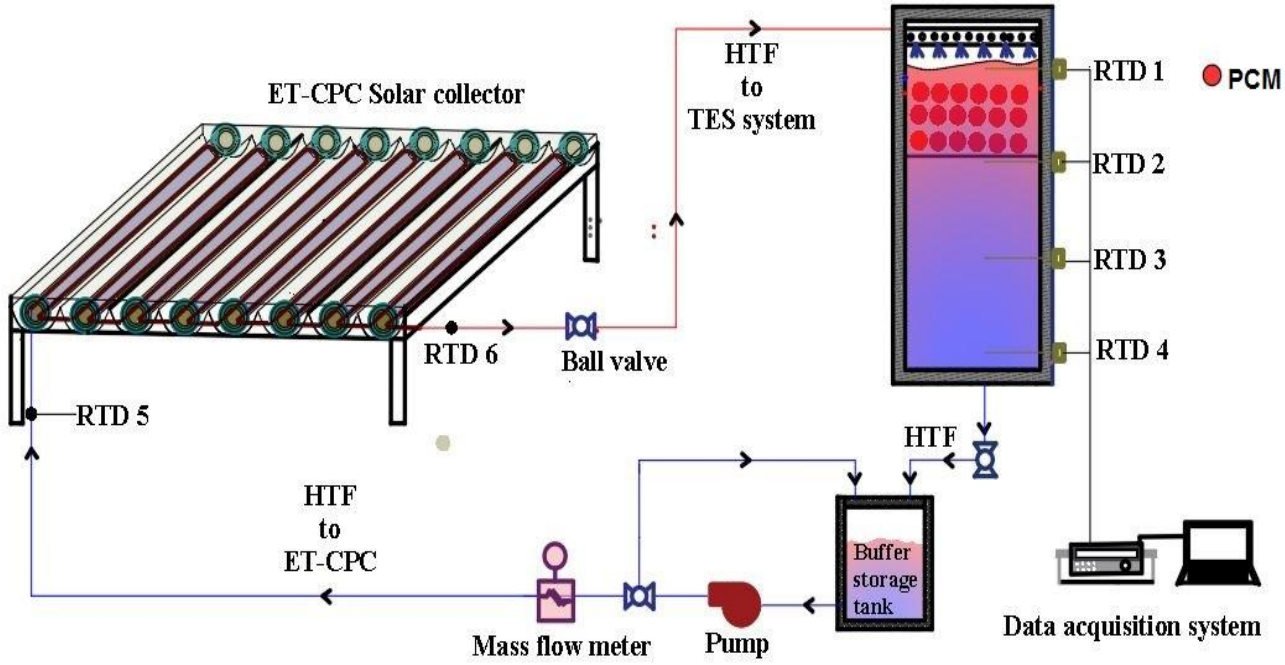

Figure 1 Schematic layout of the experimental setup

Galvanized iron was used for the construction of a cylindrical type STESS having a dimension of 0.5 m diameter and 1 m height and it was filled with 200 *l* of water. The HTF was circulated in a closed loop, and makeup water was supplied from a buffer tank of 50 *l*, positioned between the STESS and XCPCSC. Adequate space was given in the STESS to fix valves and temperature sensors. Water, the selected HTF, was circulated from the buffer tank through a copper tube in the receiver using a centrifugal pump. The mass flow rate of HTF was constantly observed using Coriolis mass flow meter (ABB, FCB300) with an accuracy of ± 0.12%. A pyranometer (Hukse flux, LPO2) was placed near the experimental facility for the measurement of intensity of solar radiation with an accuracy of ±10 W m^{-2}. Incoming HTF from the collector to STESS was uniformly distributed using the sprinklers placed at the top of STESS. Temperature sensors (RTD of Class 'B' type with an accuracy of ±0.1 °C) were placed at the inlet and outlet of XCPCSC and STESS for the measurement of HTF temperature. The energy obtained was transferred during the charging process to the fluid in the STESS. The HTF leaving the STESS was recirculated to

XCPCSC, continuing the charging cycle from 9.00 h to 16.00 h at the intended mass flow rate. The Schematic layout of the experimental setup of SWH system is illustrated in Figure 1.

2.2. TRNSYS model description

Figure 2 (a-d) is the TRNSYS flow diagram for SWH system. At the start of the simulation, HTF was pumped from the lower part of the STESS to the XCPCSC in the charging cycle. Following that, hot HTF entered in at the upper part of STESS with charging done by direct mixing of HTF with water already present in the STESS. During the discharging cycle, HTF from the makeup water tank was driven to the lower part of the STESS system, for mixing directly with hot water. With a one-hour time interval, simulations wereperformed using TRNSYS software.The simulation technique of the successive approach was taken into consideration for gettinga suitable sequential solution. The progremme was dveloped for varying the flow rate of HTF in the XCPCSC for achieving the uniform outlet temperature of 85 °C under charging conditions. Parameters considerd for analysis are given in Table 1.

Table 1 Range of design parameters

Parameter	Value
Area of solar collector	2.5 m^2, 4 m^2, 5 m^2,6 m^2, 7 m^2 and 8 m^2
Mass flow rate	30 kg h^{-1} – 240 kg h^{-1}
$F_R(\eta_o)$	0.37
F_RU_L	2.19
Volume	280 *l* – 300*l*
Length	0.6 *m*-1.6 *m*
Internal diameter	25.4 mm

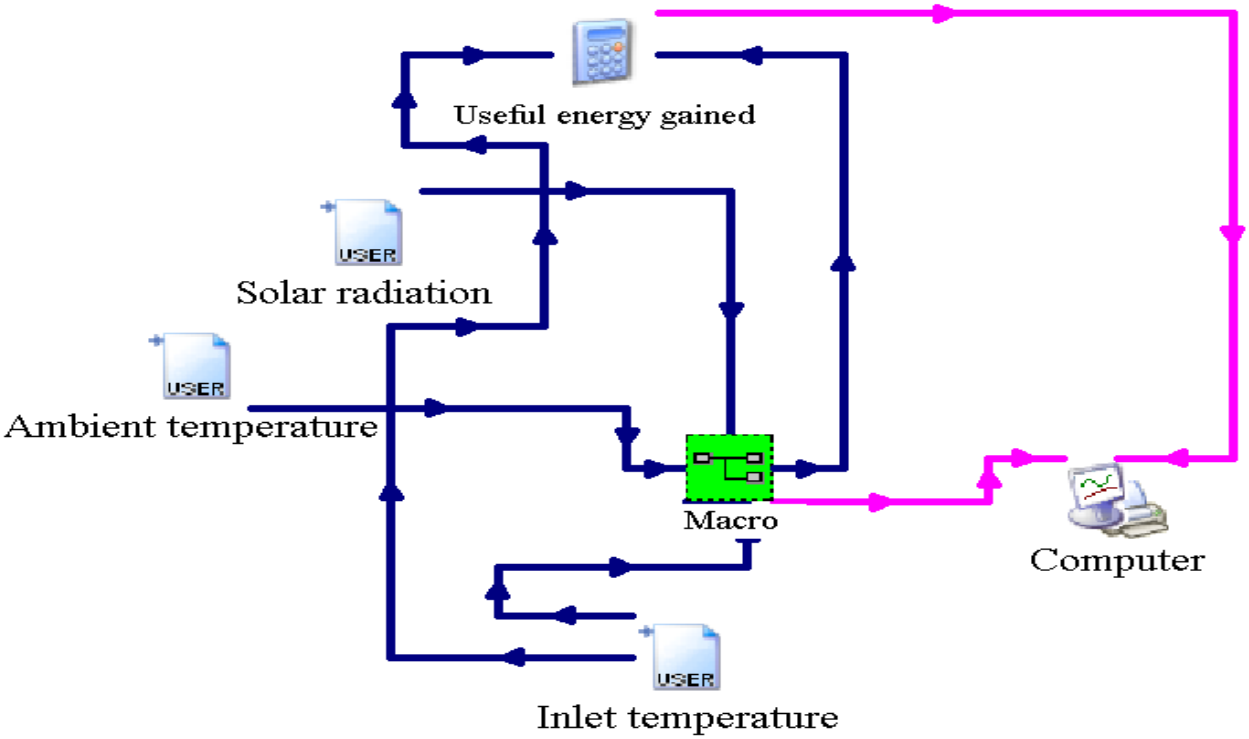
Useful energy gained
USER
Solar radiation
USER
Ambient temperature
Macro
Computer
USER
Inlet temperature

(a)

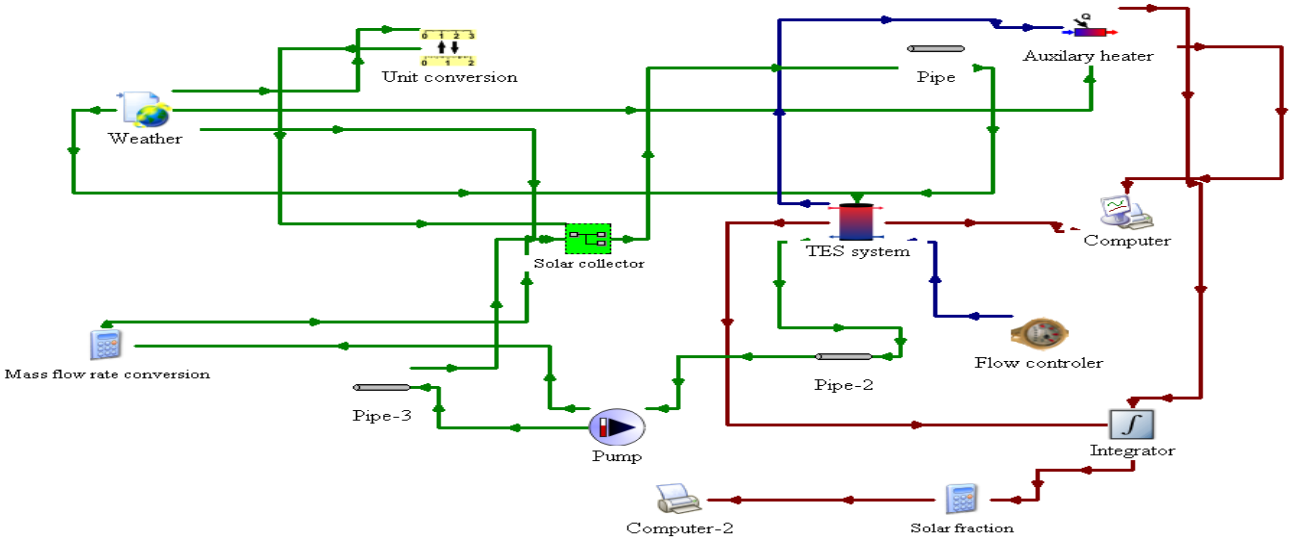
Unit conversion
Weather
Pipe
Auxilary heater
Solar collector
TES system
Computer
Mass flow rate conversion
Flow controler
Pipe-2
Pipe-3
Pump
Integrator
Computer-2
Solar fraction

(b)

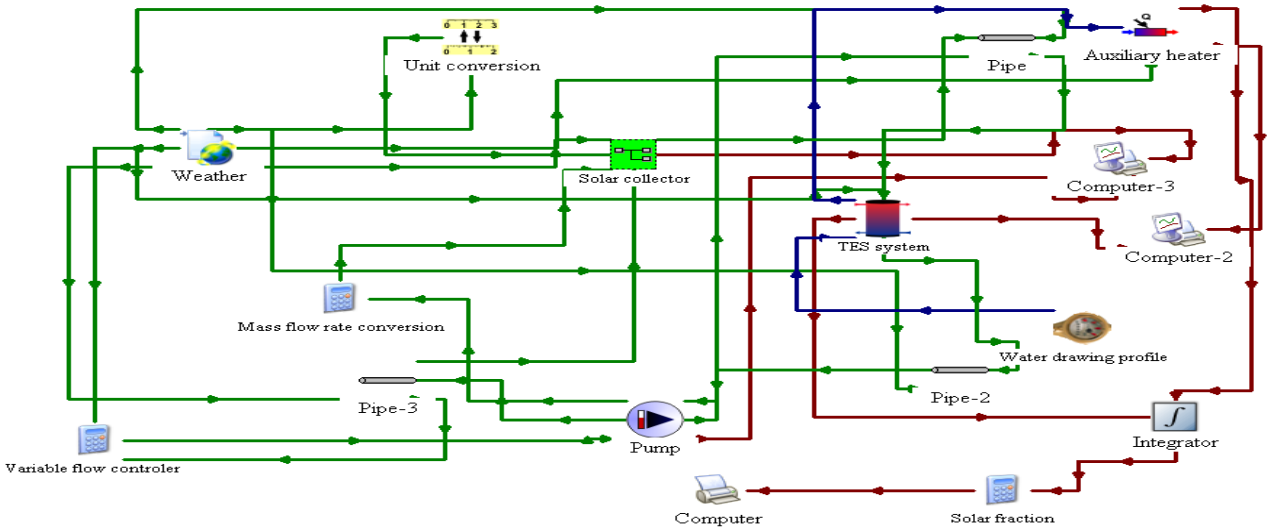

(c)

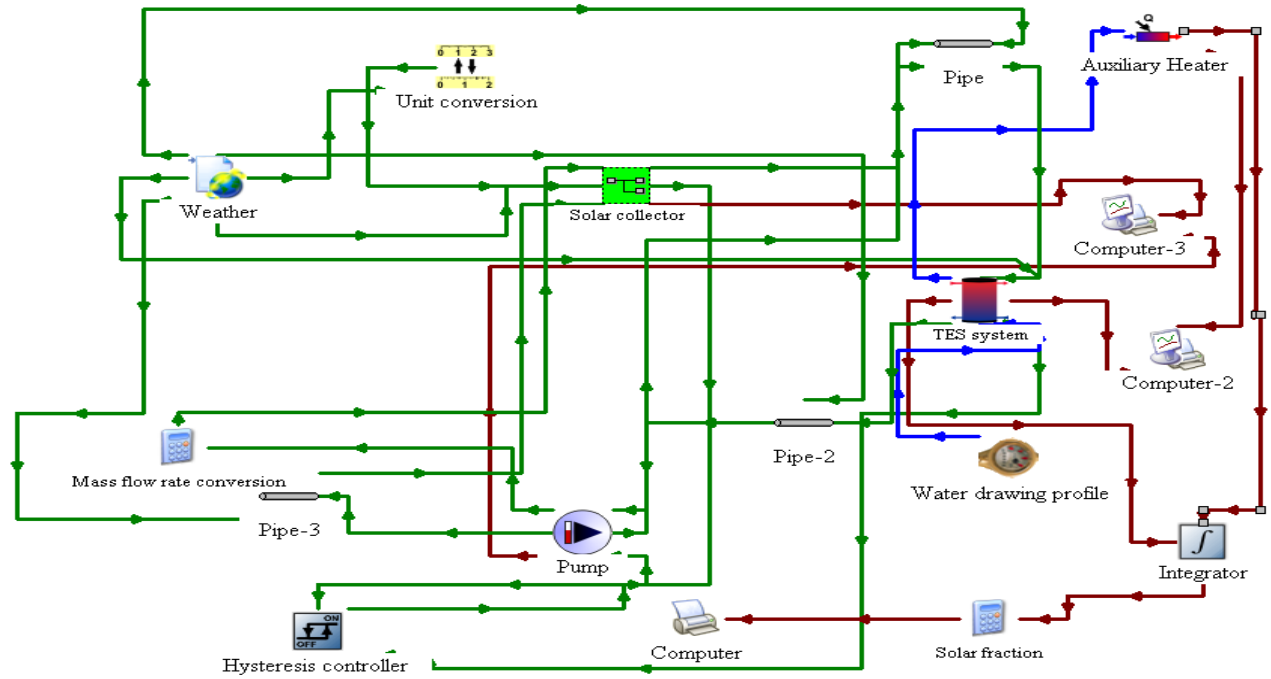

(d)

Figure 2 Flow diagram of SWH system (a) charging cycle (b) without controller (c) with variable controller (d) with hysterises controller

Depiction of the TRNSYS deck file used in the SWH system are given below:

- Data Reader for Generic Data Files (Type 9): For importing experimental data such as weather and ambinet temperature into TRNSYS platform for valdiating the developed model
- Insert new equation :Inserting user defined relations such as Eq 1-4 and algorithms for modellingand comntrolling component in the proposed system.
- STESS (Type 4): The behavior of STESS was investigated by altering the tank L/D ratio. The total heat loss coefficient is considered as2 kJ h^{-1} m^{-2} K^{-1}.
- Unit conversion (Type 57): For converting the given outputs units into appropriate right input units in the deck files.
- Forcing unit (Type 14): The file is used to execute a periodic hourly load profile depending on energy usage.
- Auxiliary heater (Type 6): Following STESS, an auxiliary heater is coupled for raising the temperature; the required HTF is preset at60 °C.
- Pump (Type 110): HTF is circulated between the XCPCSC and the STESS using a pump. This pump is operated by two different controllers namely hysteresis and variable speed.
- Pipes (Type 33): The internal pipe diameter of 25.4 mm is considered for the study. The heat loss coefficient assumed to be 3 kJ h^{-1} m^{2} K^{-1}.
- Integrator (Type 24): This file is used for periodic integration of given data.
- Output (Type 65): Visually displaying the results on periodic functions.
- Output (Type 25): Obtaining the raw data for further analysis.

3. DATA ANALYSIS

Collector efficiency in terms of optical efficiency (η_{opt}), overall loss coefficient and instantaneous solar radiation is expressed in Eq. (1-2) as given below.

$$\eta = \frac{Q_u}{Q_{in}} = F_R(\eta_{\text{opt}}) - F_R(\mathrm{U_L})\frac{(\mathrm{T}_i - T_{amb})}{I} \quad (1)$$

$$\eta = \frac{Q_u}{Q_{in}} = F_R(\eta_{\text{opt}}) - \frac{F_R(\mathrm{U_L})}{C_R}\frac{(\mathrm{T}_i - T_{amb})}{I} \quad (2)$$

where $F_R$is the heat removal factor, U_L is the overall loss coefficient (W $m^{-2}K^{-1}$), C_R is the concentration ratio, T_i and T_a are the inlet and ambient temperature (K), I is the Global radiation (W m^{-2}).

The following equation is used for the computation of the useful heat energy gained by the XCPCSC,

$$Q_u = \dot{m}_f \times c_f \times \Delta T \times dt \quad (3)$$

where, $\dot{m}_f$is HTF mass flow rate (kg h^{-1}),T_o and T_i are inlet and outlet HTF temperature (K).

The SF is evaluated using the following equation (Kalogirou, 2014).

$$SF = \frac{Q_s}{Q_S + Q_A} \quad (4)$$

where Q_S and Q_A are energy delivered from the STESS (W) and additional required energy supplied by the auxiliary component (W).

4. RESULTS AND DISCUSSION

4.1Experimental validation

Inclusion of‘ F_RU_L’ and ‘$F_R(\tau\alpha)$’is essential in the TRNSYS tool for predicting the performance of SWH system. These were determined from the Eq. (1-2). The experiments were performed at different HTF flow rates of 60 kg h^{-1}, 120 kg h^{-1} and 180 kg h^{-1} on 22 – 27 April 2022 during 9.00 h-16.00 h. In accordance with ASHRAE 93-2003 standard[22], before and after solar noon, at least four sets of replication data having a minimum of four symmetry points are required for plotting the collector thermal efficiency. The measured data of average solar radiation was 712 W $m^{-2}$with a deviation of ± 25 W m^{-2}, that falls within the limits prescribed in ASHRAE 93-200 standard (93-2003, 2003; Al-Kayiem and Lin, 2014). Evaluation of thermal performance of XCPCSC was done in terms of instantaneous thermal efficiency with a step size of 1 *h*. Slope of the line and *y*-intercepts, denoting $F_R(\eta_{opt})$ and $F_R(U_L)$ respectively, are taken from the figure and shown in Table 2.

The simulated outcomes, as seen, are in accordance with the experimental data, with a maximum variance of 8.1%.Deviation in the data could be due to the elimination of higher order in polynomial equations and the uncertainty involved in the experimentation. After ensuring the accuracy of TRNSYS model, further simulation works were performed for selection of a suitable control system amongst three considered in the analysis. In addition, the effects of a parabolic reflector in the solar collector were studied and comparison was made with the ET collector under similar test conditions. For a given collector area of 2.75 m^2, useful heat energy gained is seen as perceivably higher in the case of XCPCSC, showing 5.17 % enhancement than the ET collector**.** This can be attributed by the trough-shaped CPC solar collector, allowing the incident sun rays at an angle beyond the half acceptance angle and hitting the receivers directly. Besides, the distinctive

advantage of the XCPCSC is minimum thermal losses, which are inversely proportional to its concentration ratio.

Table 2 Ambient temperature, solar radiations, $F_R(UL)$ and F_R (η_{opt})

$\dot{m}_f$ (kg h^{-1})	Experimental date	F_RU_L	$F_R(\eta_o)$	T_{amb} (°C)	I (W m^{-2})
60	April, 22 2022	2.67	0.38	31-37	605-957
	April, 23 2022	2.26	0.38	30-37	635-1008
120	April, 24 2022	2.14	0.38	28-33	647-901
	April, 25 2022	1.83	0.36	30-37	573-955
180	April, 26 2022	2.10	0.38	32-39	479-942
	April, 27 2022	2.15	0.38	30-37	529-892

4.2 Influence of control system

Hot water consumption of 280 $l\ d^{-1}$has been considered in this study. Details relating to the simulated data of SF for the SWH system with different control systems are shown in Figure 3.As observed, the SF attains to a maximum in the months of April and May, while minimum in the month of December under all three conditions depending on the available incident solar radiation. The lowest average annual SF is 0.48 in the case of variable flow rate controller. This can be attributed to a reduction in heat energy carried by the HTF at lower flow rates, necessitating the operation of the auxiliary heater for longer duration. This type of controller causes a decrease in the HTF flow rate, when the HTF temperature reaches above 85 °C at the outlet, not capable of charging the STES system completely. Nevertheless, the SF attains 0.68 without controller and 0.71 with a hysteresis controller. The pump is put 'ON/OFF' under the condition that switching 'ON' the pump is at T_{out}-$T_{in} \geq 5$ °C, while switching 'OFF' at T_{out}-$T_{in} \leq 1$°C. This helps the HTF circulation

maintaining nearly at 60 kg h^{-1}, minimizing the heat losses considerably in the kernel components and the connecting pipes. The augmented SF results in higher energy extraction rate, showing the improved overall thermal performance of SWH system compared to other control strategies. Considering the above, further simulations have been carried out in the proposed SWH system only with the hysteresis controller and the results are presented in the following section.

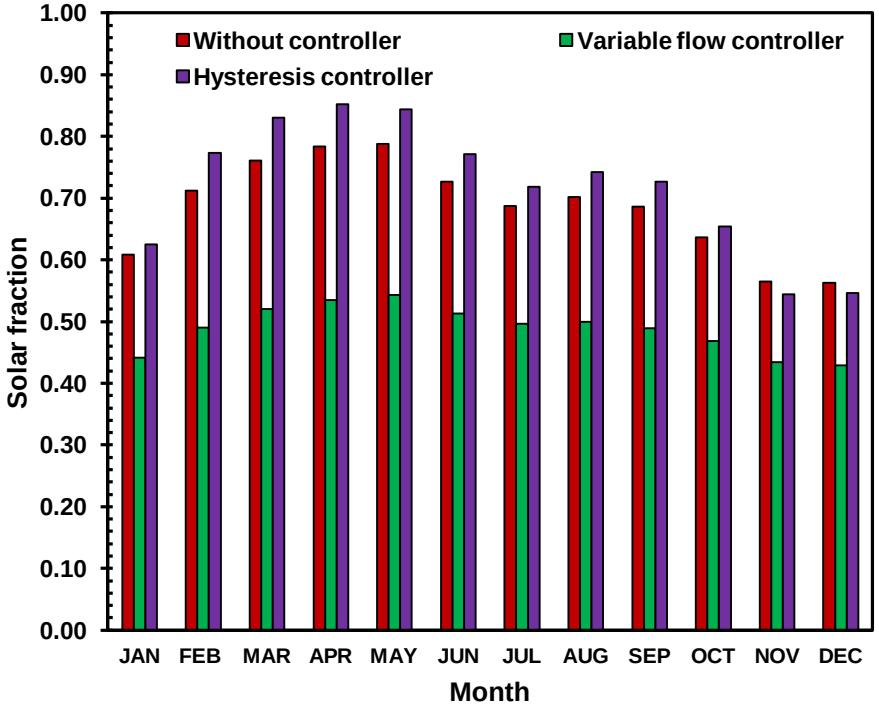

Figure 3 Solar fraction for various control systems

4.3 Variation of aperture area

The impact of an increase in the XCPCSC aperture area from 4 m^2 to 8 m^2, with an interval of1 m^2, on SF have been estimated for the same weather conditions, and the findings are given in Figure 4. To start with, the variations in SF on monthly basis are evaluated for the collector area of 2.75 m^2 and is seen as ranging between 0.65 - 0.85, as exhibited in Figure 4. Looking at the figure, monthly averaged SF of nearly 0.9 - 1 is attained for the solar collector with 8 m^2, which could be attributed to a higher useful heat energy gained in the collector for a particular available solar

radiation. An increase in average annual SF of 14 % with an enlargement in collector area from 2.75 m^2 to 4 m^2 at 60 kg $h^{-1}$is observed. As expected, the SF exhibits an increasing trend with respect to an increase in collector area due to its direct bearing on heat transfer rate. However, the trend is not in proportionate to an increase in the collector area. As perceived, SF augments only by 1.3 % for variation in the area from 7 m^2 to 8 m^2, but significantly improves by10 % when the area varies from 4m^2 to 5 m^2. On comparing the results, an insignificant gain in SF after the collector area above 6 m^2 was seen. The collector area is vital, particularly in domestic application, where the space is more constrained. Over sizing also involves redundant heat losses and higher capital cost. From the parametric analysis, the optimal collector area is taken as 6 m^2, exhibiting more sensitivity to SF without compromising on thermal performance.

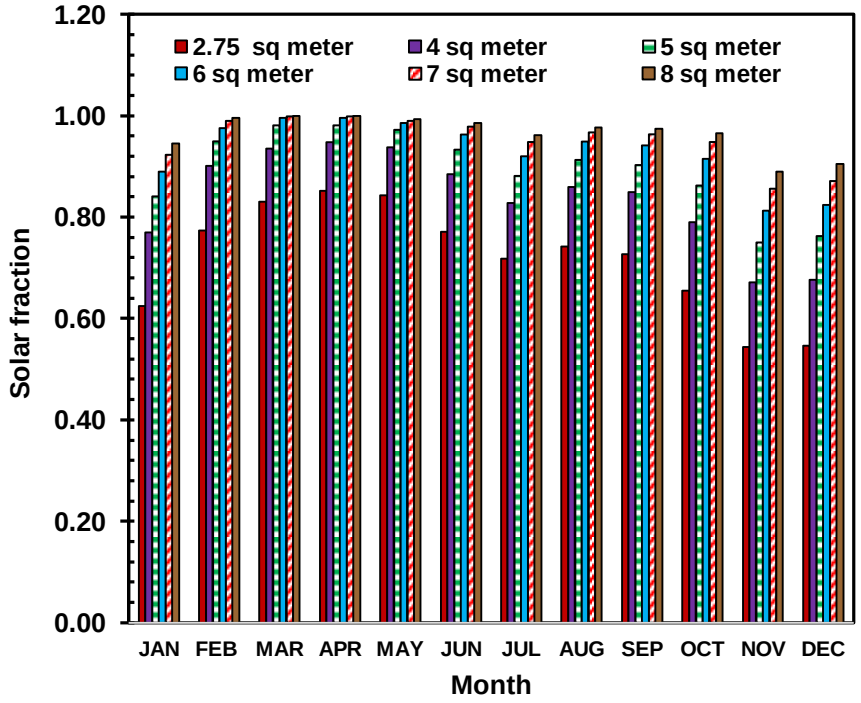

Figure 4 Monthly averaged solar fraction

4.4 Effect of mass flow rate

Figure 5 shows the SF values calculated for a collector aperture area of 6 m^2 at varied flow rates of 30 - 240 kg h^{-1}. As noticed from the figure, the monthly average SF shows the upward trend with increasing flow rate, resulting a maximum of 0.97 in the month of April. Only a modest increase in SF is seen with an increase in the flow rate, indicating the unfavorable operating conditions with regard to hot water demand. The annual average SF is incremented to a maximum of 0.87 - 0.96 as the flow rate increases from 30 kg h^{-1} - 120 kg h^{-1}. This is because of a considerable gain in energy output with increasing mass flow rate, that also reduces the associated heat losses between the solar collector and ambient. An insignificant increase in SF of only 0.5 - 2 % is seen, while the flow rate is maintained above 120 kg h^{-1}due to destratification in TES system. The HTF flow rate of 120 kg h^{-1}, which provides the most favorable SF, is evaluated for further investigation based on the previous discussion.

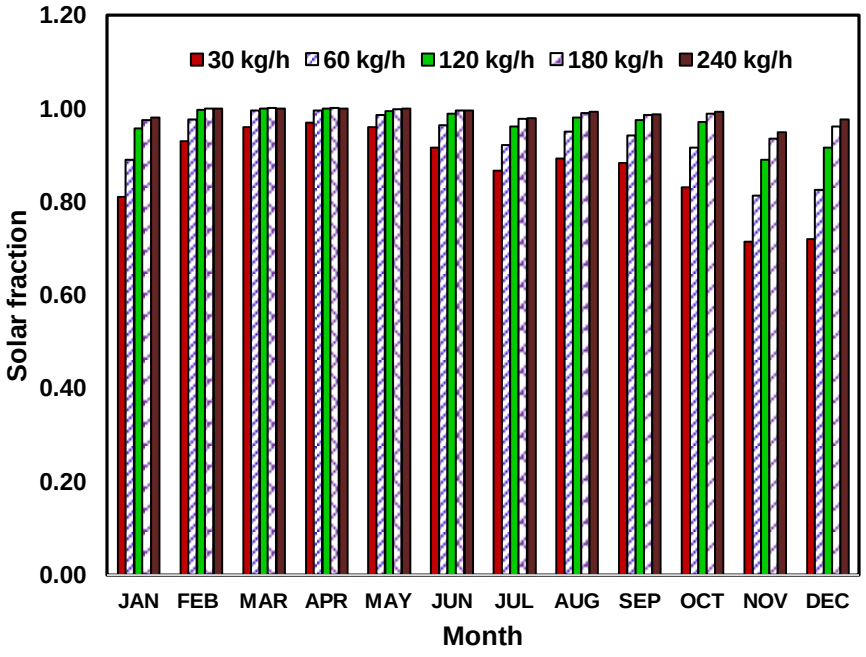

Figure 5 Solar fraction at different HTF mass flow rates

4.5 Volume and height of STESS

Flow rate of the HTF has a considerable impact on the size of STESS owing to the variation in its resident time. Firstly, keeping height of the TES system as 1 *m*, series of simulation have been

Table 3 Variation of solar fraction for TES geometry

Fixed parameter	Varying parameter	Solar fraction
$\dot{m}_f$= 120 *kg* h^{-1} L = 1 m	V=280*l*	0.960
	V=285 *l*	0.961
	V=290 *l*	0.961
	V=295 *l*	0.950
	V=300 *l*	0.945
$\dot{m}_f$= 120 *kg* h^{-1} V = 285 *l*	L = 0.6	0.900
	L = 0.8	0.940
	L = 1.0	0.961
	L = 1.2	0.965
	L = 1.3	0.967
	L = 1.4	0.968
	L = 1.5	0.968
	L = 1.6	0.969
	L = 1.7	0.970
	L = 1.8	0.972

carried out with variations in the volume of the STESS between 280 - 310 *l*and the corresponding results are presented in Table 3. As expected, a negligible change in SFis observed up to 290 *l*. However, further increase in volume of TES results in a reduced SF, which could be attributed to a higher heat infiltration from the STESS. For the considered simulation, the variation inSFshowsa declining trend above 290 *l* and so an average TES volume of 285 *l*is taken for theanalyses ofthe effects of the height of the TES system. As seen from Table 3, on increasing the height from 0.2 m

to 1.2 m augments the SF from 0.9 to 0.97, owing to better thermal stratification resulting from a higher aspect ratio of STESS. This effect is almost insignificant, when the height of STESS is above 1.2 m, exemplifying the fully stratified behavior of STESS. On this basis, the STESS of 1.2 m height and 285 *l*volume is seen as the favorable option compared to the other cases for better utilization of solar energy.

5. CONCLUSIONS

Analysis of thermal performance of SWH paired with STESS was made under transient conditions using TRNSYS for the whole year. The major design and operating parameters of SWH system were evaluated under climatic conditions of Chennai. Water was circulated for transferring heat from the solar collector to the STESS, catering to a hot water demand of 280 ld^{-1}. The experimental and numerical results were found to be relatively close, establishing the validity of the TRNSYS model. Monthly averaged solar fraction of SWH system using hysteresis controller exhibits a better performance. A maximum increase in solar fraction of 26.3 % is obtained with an increase in the aperture area from 2.75 m^2 to 6 m^2 at a constant HTF flow rate and further increase in area has almost no effect on solar fraction. Based on that, the HTF mass flow rate is optimized as 120 kg h^{-1}, performing better in the month of April and May and reaching an annual average solar fraction of 0.96. Simulations carried out enable designing the volume and height of STESS as 1.2 m and 285 *l* for attaining a higher degree of thermal stratification, thereby augmenting the thermal performance of XCPCSC. The proposed system is capable of supplying hot water even during the night hours, meeting the major challenges seen in the other SWH systems, particularly for buildings. In conclusion, SWH system can be sized on the basis of solar fraction arrived at from the satisfactory prediction of long term performance using the TRNSYS model. Multi-design optimization and smart control strategies in SWH system for improving its thermal performance remain to be explored.

NOMENCLATURE

c_p	liquid specific heat (J kg^{-1} K^{-1})
C_R	concentration ratio
D	least value of experimental parameters
F_R	heat removal factor
I	solar radiation (W m^{-2})
$\dot{m}_f$	mass flow rate (kg s^{-1})
Q	heat energy gained(kJ)
U_L	overall loss coefficient (W m^{-2} K^{-1})
η	Thermal efficiency
X	mass flow rate fraction

SUBSCRIPTS

amb	ambient
AUX	auxiliary
o	outlet
opt	optical
i	inlet
SOL	solar energy
u	useful

ABBREVIATIONS

CPC compound parabolic concentrator

ET evacuated tube

FPC flat plate collector

HTF heat transfer fluid

PCM phase change material

SWH solar water heating

SF solar fraction

STESS Sensible thermal energy storage system

References

93-2003, A.S., 2003. Methods of testing to determine the thermal performance of solar collectors. Atlanta, GA, USA.

Abdunnabia, M.J.R., Alakder, K.M.A., Alkishriwi, N.A., Abughres, S.M., 2014. Experimental validation of forced circulation of solar water heating systems in TRNSYS, in: Energy Procedia. Elsevier Ltd, pp. 2477–2486. https://doi.org/10.1016/j.egypro.2014.10.257

Al-Kayiem, H.H., Lin, S.C., 2014. Performance evaluation of a solar water heater integrated with a PCM nanocomposite TES at various inclinations. Sol. Energy 109, 82–92. https://doi.org/10.1016/j.solener.2014.08.021

Antoniadis, C.N., Martinopoulos, G., 2019. Optimization of a building integrated solar thermal system with seasonal storage using TRNSYS. Renew. Energy 137, 56–66. https://doi.org/10.1016/j.renene.2018.03.074

Arab, M., Abbas, A., 2013. Model-based design and analysis of heat pipe working fluid for optimal performance in a concentric evacuated tube solar water heater. Sol. Energy 94, 162–176. https://doi.org/10.1016/j.solener.2013.03.029

Christopher, S., Kumaresan, V., Raghavan, K.S., 2021. Role of thermal energy storage for enhancing thermal performance of evacuated tube with compound parabolic concentrator collector. Int. J. Energy Res. 45, 7341–7351. https://doi.org/10.1002/er.6318

Dinçer, I., Rosen, M.A., 2010. Thermal Energy Storage: Systems and Applications, Second Edition, Thermal Energy Storage: Systems and Applications, Second Edition. Wiley. https://doi.org/10.1002/9780470970751

Gang, P., Guiqiang, L., Xi, Z., Jie, J., Yuehong, S., 2012. Experimental study and exergetic analysis of a CPC-type solar water heater system using higher-temperature circulation in winter. Sol. Energy 86, 1280–1286. https://doi.org/10.1016/j.solener.2012.01.019

Guédez, R., Spelling, J., Laumert, B., Fransson, T., 2014. Optimization of thermal energy storage integration strategies for peak power production by concentrating solar power plants, in: Energy Procedia. Elsevier Ltd, pp. 1642–1651. https://doi.org/10.1016/j.egypro.2014.03.173

Hankins, M., 2012. Stand-alone Solar Electric Systems: "The Earthscan Expert Handbook for Planning, Design and Installation" (Google eBook).

Hobbi, A., Siddiqui, K., 2009. Optimal design of a forced circulation solar water heating system for a residential unit in cold climate using TRNSYS. Sol. Energy 83, 700–714. https://doi.org/10.1016/j.solener.2008.10.018

Kalogirou, S.A., 2014. Solar Energy Engineering: Processes and Systems: Second Edition, Solar Energy Engineering: Processes and Systems: Second Edition. Elsevier Inc.

https://doi.org/10.1016/C2011-0-07038-2

Kürklü, A., Özmerzi, A., Bilgin, S., 2002. Thermal performance of water-phase change material solar collector. Renew. Energy 26, 391–399. https://doi.org/10.1016/S0960-1481(01)00130-6

Li, G., Pei, G., Su, Y., Ji, J., Wang, D., Zheng, H., 2016. Performance study of a static low-concentration evacuated tube solar collector for medium-temperature applications. Int. J. Low-Carbon Technol. 11, 363–369. https://doi.org/10.1093/ijlct/ctt083

Liu, Z.H., Hu, R.L., Lu, L., Zhao, F., Xiao, H.S., 2013. Thermal performance of an open thermosyphon using nanofluid for evacuated tubular high temperature air solar collector. Energy Convers. Manag. 73, 135–143. https://doi.org/10.1016/j.enconman.2013.04.010

Shrivastava, R.L., Kumar, V., Untawale, S.P., 2017. Modeling and simulation of solar water heater: A TRNSYS perspective. Renew. Sustain. Energy Rev. https://doi.org/10.1016/j.rser.2016.09.005

Sokhansefat, T., Kasaeian, A., Rahmani, K., Heidari, A.H., Aghakhani, F., Mahian, O., 2018. Thermoeconomic and environmental analysis of solar flat plate and evacuated tube collectors in cold climatic conditions. Renew. Energy 115, 501–508. https://doi.org/10.1016/J.RENENE.2017.08.057

Tchinda, R., Ngos, N., 2006. A theoretical evaluation of the thermal performance of CPC with flat one-sided absorber. Int. Commun. Heat Mass Transf. 33, 709–718. https://doi.org/10.1016/j.icheatmasstransfer.2006.01.019

Tiwari, A.K., Gupta, S., Joshi, A.K., Raval, F., Sojitra, M., 2020. TRNSYS simulation of flat plate solar collector based water heating system in Indian climatic condition. Mater. Today Proc. https://doi.org/10.1016/j.matpr.2020.08.794

TRNSYS primary [WWW Document], 2021. URL https://sel.me.wisc.edu/trnsys/weather/weather.htm (accessed 6.29.21).

Xia, E.-T., Chen, F., 2020. Analyzing thermal properties of solar evacuated tube arrays coupled with mini-compound parabolic concentrator. Renew. Energy 153, 155–167. https://doi.org/10.1016/j.renene.2020.02.011

Xu, J., Chen, F., Xia, E., Gao, C., Deng, C., 2020. An optimization design method and optical performance analysis on multi-sectioned compound parabolic concentrator with cylindrical absorber. Energy 197, 117212. https://doi.org/10.1016/j.energy.2020.117212